New Schiff Bases as Corrosion Inhibition and Biological Activity of Their Metal Complexes

Tahani I. Kashar, Khadijah M.Emran

***Abstract*— Corrosion inhibition of N-(2-hydroxyphenyl)-3-(2-hydroxyphenylimino) butanamid (H2L1) and ethylacetoacetate-isonocotinoyl thiosemicarbazied hydrazone (H2L2) were evaluated. The inhibition efficiencies obtained from both MLM and HEM methods are in good agreement. Defferences in inhibition efficiency between H2L1 and H2L2 are correlated with their chemical structures. Temkin isotherm is found to provide an adsorption description of Schiff bases. The Palladium(II), mercury(II), cadimum(II) and zinc(II) complexes have been synthesized and characterized by EA, IR, UV–Vis spectra, molar conductances, 1H NMR , mass spectra and thermal analyses (DTA,TG) measurements. The IR data of complexes of the ligand (H2L1) suggested that it coordinated to the metal ions as bi or tridentate. The complexes of the ligand (H2L2) suggest the involvement of sulfur and azomethine nitrogen atoms in coordination to the central metal ion. The Molar conductances of the complexes in DMF are agree with their non-ionic character for the complexes of the ligand (H2L1) and ionic for the complexes of the ligand (H2L2). Electronic spectral studies indicate an octahedral geometry for the Cd(II),Hg(II) and Zn(II) complexes while square planar geometry for the Pd(II) complexe of the ligand(H2L1).The ligands and their metal complexes were tested for their antimicrobial activities. The activity show that the complexes are more active antimicrobials than the ligands.[(HL1)2Hg(H2O)2]2H2Ocomplex showed higher range of inhibition diameter than Ampicillin , Amphotericin B and other complexes.**

***Index Terms*— Synthesis, Corrosion inhibition properties, Transition metal complexes**

I. INTRODUCTION

Cast iron has been used extensively in many industrial applications, such as water industry, for more than 150 years[1,2]. However, cast irons have relatively low impact resistance for corrosion in acidic media[3,4]. Generally corrosion inhibitors are organic compounds containing electronegative atoms (such as N, S, P and O), unsaturated bonds, and conjugated systems including all kinds of aromatic cycles [5–11]. Schiff bases have inhibition efficiency greater than that of corresponding amines and aldehydes. This due to the presence of a C=N group in the molecules [12–14]. The most advantages of these surfactant inhibitors are high inhibition efficiency of them, low price, low toxicity and easy production [15-18]. Schiff bases have many extensive applications in medicinal, pharmaceutical fields, agricultural and material science [19,20]. Due to their easily preparing procedures and their ability to attach to several functional groups on their chemical structure, Schiff bases are considered good bases for synthesis of many antibacterial compounds [21]. The condensation of aliphatic diamines such as ethylenediamine or its derivatives with salicyaldehyde result tetradentate Schiff bases. These compound especially those with the N_2O_2 donor have been extensively studied [22]. Schiff bases derived from aromatic diamines have received much less attention. Condensation of isonicotinic acid hydrazide with aldehydes produce Hydrazones derived. These Hydrazones derived found to show better antitubercular activity than INH (INH is a drug used against a wide spectrum of bacterial ailments) [23].The aim of the present investigation was to synthesis an examine both the inhibitive action of N-(2-hydroxyphenyl)-3-(2-hydroxyphenylimino) butanamid and ethylacetoacetate isonocotinoyl thiosemicarbazied hydrazone towards the corrosion of cast iron in 2M HCl and their application for syntheses and characterization of new Palladium(II), mercury(II), cadimum(II) and zinc(II) complexes as well as screening for their antimicrobial activities.

Manuscript received Aug 15, 2016

Tahani I. Kashar, Department of Chemistry,, College of Arts and Science, Qassim University, Saudia Arabia

Khadijah M.Emran, Department of Chemistry, College of Science ,TaibahUniversity, Madina Monawara, Saudia Arabia

II. EXPERIMENTAL DETAILS

2.1Material and Solutions

All chemicals and solvents used were pure chemicals from BDH or Aldrich and used as received. Corrosion tests were performed on cast iron specimen with weight percentage compositions in **Table 1**. The cast iron specimens were purchased from ATTAIH Company.

2.2 Synthesis of the ligands

For preparation of the ligands N-(2-hydroxyphenyl) -3-(2-hydroxyphenylimino) butanamid (H_2L^1), hot ethanolic solutions of ethylacetoacetate(0.01mol) and 2-aminophenol (0.02 mol) were mixed and refluxed for 3 hours on a water bath. The resulting solution was concentrated and cooled in an ice bath. The separated precipitate was collected through filtration using a vacuum pump and washed with ethanol, dried over anhydrous calcium chloride. The melting point was determined and found to be 185°C.

For preparation of the ligandethylacetoacetateisonocotinoyl thiosemicarbazone(H_2L^2).The ligand was prepared by refluxing the ethanolic solution containing equal moles of ethylacetacetate and thiosemicarbazide for three hours on awater bath. The refluxed solution was concentrated and separated by filtration and washed with ethanol. Hot ethanolic solutions of ethylacetoacetatethiosemicarbazone(0.01mol) and isonicotinic acid hydrazide (0.01 mol) were mixed and refluxed for 2 hours on a water bath. The separated precipitate

filtered ,dried over anhydrous calcium chloride in a desiccator. The melting point of it was found to be 110°C.

2.3 Synthesis of the complexes

The hot ethanolic solutions of corresponding metal salt (0.05mol), ligands (H_2L^1 orH_2L^2) (0.05mol) were mixed and refluxed for about 3-5 hours to get theZn(II),Cd(II),Hg(II) and Pd(II) metal complexes. The refluxed solution was cooled for overnight and filtered. The obtained metal complexes dried in a desiccators over anhydrous calcium chloride.

2.4 Measurements

Elemental analyses (EA) (C, H, N, Cl and S) were determined using atomic absorption with a Perkin Elmer (model 2380) spectrophotometer. The IR spectra using a Perkin-Elmer 1430 infrared spectrometer were measured as KBr discs in range 4000-200 cm^{-1}. Electronic absorption spectra in the 200-900 nm region were recorded on a Perkin-Elmer 550 spectrophotometer. The thermal analyses (DTA and TGA) were carried out in the 27-800^oC range at a heating rate of 10$^oC.min^{-1}$ by a Shimadzu DT-30 and TG-50 thermal analyzers. The Gouy method with mercuric tetrathiocyanatocobaltate(II) as magnetic susceptibility standard were used to measure magnetic susceptibilities at room temperature. Diamagnetic corrections were made using Pascal's constants. A BibbyconductimeterMCl was used for conductance measurements.

Corrosion measurements were carried out by hydrogen evolution measurement (HEM), and mass loss measurement (MLM). The loss in weight was calculated from the difference between the before and after the experiment weights. Duplicate experiments were performed in each case and the mean value of the mass loss and hydrogen evolution was determined. The temperature was adjusted at 27°C by thermostat.

2.5 Antimicrobial activity

The ligands and their metal complexes were tested for their in vitro antibacterial activity against Escherichia coli, Staphylococcus aureus and antifungal activity against A spergillusflavus and Candida albicans using a modified Kirby- Bauer disc diffusion method[24]. A mpicillin (Antibacterial agent) and A mphotericin B (Antifungal agent) served as positive controls for antimicrobial activity. For negative control, filter discs impregnated with 10 µl of solvent DMSO were used. For the disc diffusion the zone diameters were measured with slipping calipers of the National Committee for Clinical Laboratory Standards [25].

III. RUSLTES AND DISCUSSION

Prepared metal complexes are stable at room temperature. They were non hygroscopic, partially soluble in methanol or ethanol and more soluble in DMF and DMSO. The analytical data for the ligands and metal complexes are compatible with their proposed molecular formula. The molar conductivity data (**Table2**) of the complexes indicates that all the metal complexes are non electrolytes of the ligand (H_2L^1) while the complexes of the (H_2L^2) are electrolytes.

3.1 ^{1}HNMR and ^{13}C- NMR spectra.

The NMR spectra of the ligandH_2L^1 show different signals (**Table 2**) at δ 9.0 ppm (NH), 4.5ppm(OH) and 6.4-7.0 ppm aromatic proton and a singlet at δ3.5,2.5ppm corresponds to CH_2 andCH_3 protons respectively[26].These signals are not changed in the NMR spectra of its Cd(II) complexe indicating that these peaks don't participated in coordination with the cadmium.The^{1}H-NMR spectrum ofethylacetoacetateisonocotinoylthiosemicarbazone$H_2L^2$was recorded in DMSO solvent. It shows signals corresponding to CH_3,CH_2 and -OH protons at 1.1 (tri.3H), 4.1 (quar., 2H), 10.1 (OH) and doublet signals appeared at 7.7 and 7.8 ppm corresponding to pyridyl protons. The NMR spectrum of its Cd(II) complex confirms coordinated with metal ion through ketonic oxygen atom of isonicotinic acid hydrazide.

^{13}C- NMR spectra were recorded in DMSO of the ligand (H_2L^2),178.9(C=S); 169.4(C=O); 150.4.73(C=N) ; 147.1(CH-py); 121.2(C-H-py); 60.6(CH2), 16.6(CH_3), 13.9(CH_3).

3.2 Infrared spectral studies of the ligand N-(2-hydroxyphenyl) -3-(2-hydroxyphenylimino) butanamid (H_2L^1) and its complexes.

The characteristic IR absorption bands of the ligand and it scomplexes are summarized in**Table4**. The comparison of the in fraredspectra of the complexes and the ligand (H_2L^1)reveal that the spectra of complex esdifferfrom that of the ligand in some characteristic frequencies. A strong intense and appears at 1588cm^{-1} in the spectrum of the ligand due to νC=Nvibrations, **Fig.(1)** has undergone a frequency shift of about 20-15 cm^{-1} in all metalcomplexes, this shift indicates the coordination of nitrogen to metalion[27].The band at 1727cm^{-1} is characteristic of the C=O in the free ligand disappearance in the complexes indicates the coordination of the oxygen of keto group through enolic form. The presence of the -OH group in the ligand at 3481 cm^{-1}. This band is absent in metal chelates which mean that one group of the -OH is involved in the coordination[28]. The aromatic out of plane vibration is seen near 870 $cm^{-1}$and in plane vibration at 770$cm^{-1}$and 725 cm^{-1}.Conclusive evidence of bonding of the ligand to the central metal ion is provided by the appearance of bands at ~600 $cm^{-1}$and~ 530 cm^{-1}, which assigned to M-O and M-N bands respectively[29]. Coordinated water molecules that presence in the complexes is confirmed by the appearance of band between 3250-3415 cm^{-1} and is followed by a sharp rocking mode of vibration between 840-850 cm^{-1}[30].

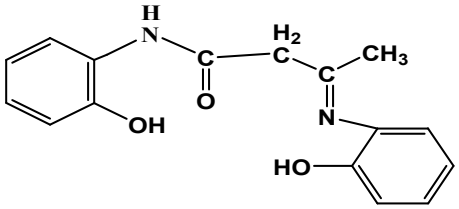

Fig .1: Structure of the ligand (H_2L^1)

3.3Infrared spectral studies of the ligandethyl acetoacetate isonocotinoyl thiosemicarbazone(H_2L^2) and its complexes

The important infrared absorption frequencies obtained for the ligand $H_2L^2$and its complexes are given in the **Table 4**. IR spectra of the ligandshow bands at 1664 and 742cm^{-1} corresponding to C=N and C=Sstretching respectively[30]. In the IR spectra of ligands, in the region 2500-2600 cm^{-1} , due

to absence of the υ(S-H) stretching indicate that the ligand retain their thione form in the solid state. This is further inferred from the presence of a peak at 742cm^{-1} due to the υ(C=S). The ligand may be exists in keto (I) and enol (II) forms **Fig.2**.The IR spectra suggests that the coordination occurs through the azomethine nitrogen, enolic oxygen of isoniazideandthioketosulphuratomexcept Cd(II) and Zn(II) complexes. The υ(C=S) in the latter complexes shifted to lower frequency these indicating theinvolvement of the thione sulfur in complexes formation. The band appeared at1664 cm^{-1} in the ligand is lower shifted in complexes revealing the coordination of the azomethine nitrogen atom[31] in coordination .Also the bands at 1065,1025,835 and 754cm^{-1} assigned to the ν(c=s)band are lower shifted indicating the sulphur coordination to the metal ion[32]. New bands are observed in far IR spectra of metal complexes at~541 and 340cm^{-1} regions due to ν(M-N) and ν(M-S) respectively. The IR spectra of the complexes showed a broad band at 3425-3375cm^{-1} that can be assigned to the νa(OH) and νs(OH) vibration modes from watermolecules.The presence of coordinated water was confirmed by the mediumstrength bands at 840–850 cm^{-1}, characteristic of (H_2O) frequencies. The sebands were not observed in the spectra of the ligand[33].

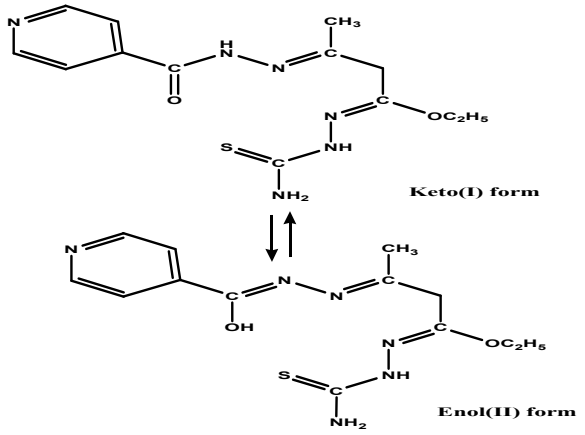

Fig .2: Structure of the ligand (H_2L^2)

3.4 Mass spectra

The mass spectra of the ligands gave the peaks at m/z 284and 322 these values consistent and proofed the molecular weight of the ligands calculated .The ions support the proposed composition and structure Fig1and2.

3.5 Electronic Spectra

The electronic transition study of the free ligands was carried out in DMF(**Table 5**). Three distinct bands were observed at291 - 226 nm; 346 - 300 nm and 433,414 nm. The first two bands are attributed to benzene π-π* and (C=N) n-π* transitions, respectively[34,35]. The absorption band at above 400 nm has been previously assigned to the keto-imine form of ortho – hydroxyl of the ligand (H_2L^1) in polar solvents [36]. Another new peaks appeared at 502 nm in its complexes reveailng the complexation occurred via ligand-to-metal charge transfer (LMCT) transition[36]. In complexes of the ligand H_2L^2 showed two major peaks. Transition of n-π* occur at the first peak at 270-287 nm, which has hyperchromic shift suggested the free imino (>C=N) group coordinated to metal atoms [37].

3.6 Molar conductivity

The molar conductivity measurements have been demonstrated to be a very useful tool in the investigation of geometrical structure of inorganic compounds. Molar conductivities of the prepared complexes were measured in 10^{-3} M DMF solutions at room temperature (**Table 3**). The complexes of the ligand (H_2L^1) showed a lower molar conductivity values in the range10.5 and 14.5 ohm^{-1}cm^2 mol^{-1}.It was concluded that the complexes are non electrolytic in nature[38]. The molar conductance value suggested that the anions were inside the coordination sphere and bonded to the metal ion. While the complexes of the ligand (H_2L^2)shows the value of molar conductance 90.5and 30.5 ohm^{-1}cm^2 mol^{-1}, which indicates the electrolytic nature, the chloride ion present in outer coordination sphere.

3.7 Thermal Study of Complexes

Thermogravimetric analysis (TGA) and differential thermal analysis (DTA) techniquesare used to determine the decomposition nature of the complex. The samples were heated up to 1000^{0}C. The calculated mass losses of the decomposition reactions are given in the **Table5**.The thermogram of complexes showed weight losscorresponding to lattice watermolecule in the range from room temperature to 150^{0}C while the loss of water in the temperaturerange above 150^{0}C(160-250^{0}C) indicates the presence of coordinated water molecule.Decomposition reaction corresponds to Cl_2 in complexes[$HL^2Zn_2.Cl.H_2O$]Cl_2 and [$H_2L^2Hg.2H_2O$] $Cl_2.2H_2O$ occurs in the temperaturerange 270-350^{0}C. Finally 600-1000^{0}C residue is obtained corresponding metal oxide as stable residue.

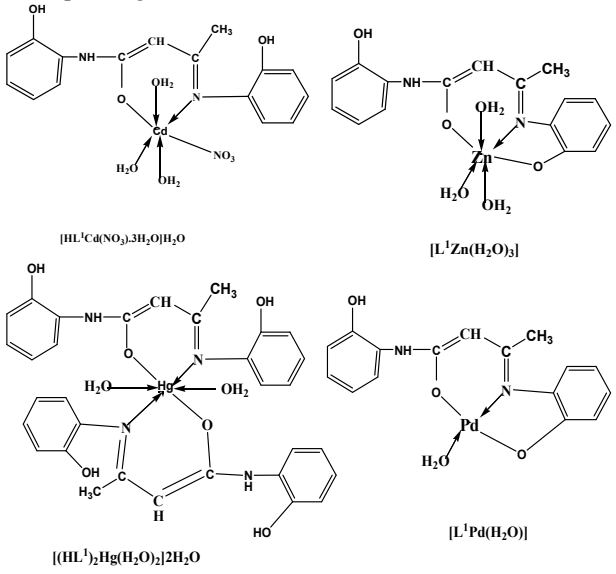

Fig.3: Structure of the complexes of the ligand (H_2L^1)

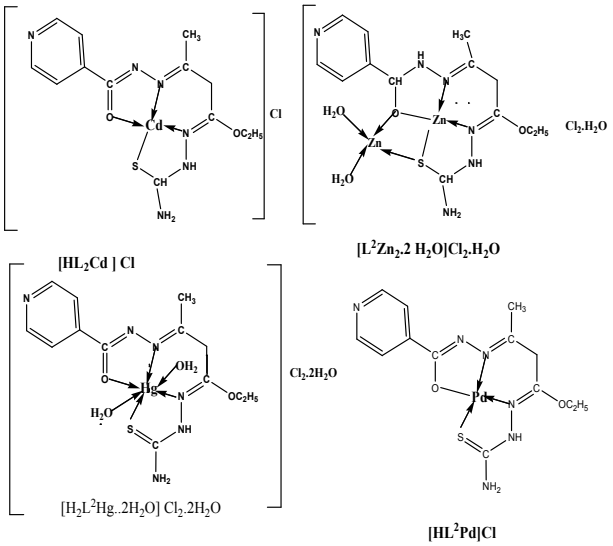

Fig.4: Structure of the complexes of the ligand (H_2L^2).

3.8 Corrosion Inhibition effect of H_2L^1 and H_2L^2

gasometric technique is a rapid and reliable means for determining the inhibitive capabilities of inhibitors on cast iron corrosion in acidic media. In many literature[39-41], gasometric technique have been established because its suitability for monitoring in situ, any perturbation by an inhibitor with respect to gas evolution in metal/solution systems. Because this technique is based on that hydrogen gas as one of iron and HCl reaction products (cathodic reaction). So, it is easier to infer that the rate of reaction corresponds to the rate of corrosion damage of the iron in HCl, which is proportional to the rate of corrosion [42].

Gasometric methods was carried out at 27°C using a gasometer. Also can be monitored in the presence of $\mathbf{H_2L^1}$or $\mathbf{H_2L^2}$as inhibitors. In each case, the metal coupon was introduced into the mylius cell (containing the test solution) of the gasometer. The rate of R_{HEM}, ml/cm^2.min) was calculated according to **Eq.1** from the slope of the graph of gas volume (V) per surface area (A) at versus time (t) as shown in **Fig. 5** according to **Eq.1**.

$$R_{HEM} = \frac{\Delta V}{\Delta t} \qquad (1)$$

A keen observation of **Fig.5,a,b** and the data in **Table 6** show that the corrosion rate of as indicated by the amount H_2 evolution slowdown in the presence of $\mathbf{H_2L^1}$or $\mathbf{H_2L^2}$ compounds when compare to 2M HCl+10% MeOH.

The calculated data from Gravimetric technique using **Eq.2**and corrosion rate(C.R) in (mmy)**, Eq.3,** of cast iron an absence and presence of $\mathbf{H_2L^1}$or $\mathbf{H_2L^2}$ are listed in **Table 1.**

$$R_{MLM} = \frac{W}{St_f} \qquad (2)$$

$$C.R(mmy) = \frac{87.6W}{StD} \qquad (3)$$

W is the weight loss of the metal (mg), *S* is the specimen area (cm^2), t is the exposure time (h) for *mmy* measurement and D is the density of the metal (g/cm^3). As can show from the data in 2M HCl+10% MeOH solution, the presence of $\mathbf{H_2L^1}$ or $\mathbf{H_2L^2}$ causes a remarkable decrease in the corrosion rate(R_{MLM} and *mmy*) compared in the presence of Schiff base when compared to the blank. Several authors have reported on comparable agreement between weight loss method and other techniques of corrosion observation include hydrogen evolution [43-44].

Values of inhibitor surface coverage (θ) and efficiencies (%EI)obtained from gasometric and gravimetric measurements using **Eq. 4** and **5** respectively are also presented in**Table 6**.

$$IE_{HEM}\% = \frac{Ro - R_{inh}}{Ro} \times 100 \qquad (4)$$

$$\theta = \frac{Ro - R_{inh}}{Ro} \qquad (5)$$

where $R_{inh.}$ is the corrosion rate at time t for inhibited solution and R_o the corrosion rate at time t for uninhibited solution.

The inhibition estimated to be superior to 73.5% and 73.2%at 1.0×10^{-2} M $\mathbf{H_2L^1}$in2M HCl+10% MeOH by HEM and MLM respectively. In case $\mathbf{H_2L^2}$**,** optimumconcentration for maximum efficiency is found to be 94.3% and 93.33% at 1.0×10^{-2} M by two methods respectively in acid medium. Good agreement was observed between the results obtain from both methods. Inspection of, **Table 6** shows that as the inhibitors concentration is raised ,the weight loss become low (*mmy*) while the %EI and θ increases. This indicate the augmentation of the number of adsorbed molecules at the cast iron. At the same inhibitors concentration the percentage of inhibition efficiency decreases in the following sequence.

$H_2L^2 > H_2L^1$

3.9Adsorption isotherm and thermodynamiccalculations

Adsorption characteristics were studied to clarify and better understanding of the organo-electrochemical reactions process on the metal surface. A quasi-substitution process between the organic inhibitor in the solution, $Org_{(sol)}$, and water molecules at the electrode surface, $H_2O_{(ads)}$, **Eq.6**, This phenomenon regarded as adsorption of inhibitor molecules from an aqueous solution on the solid state.

$$Org_{(sol)} + xH_2O_{(ads)} \rightleftharpoons Org_{(ads)} + xH_2O_{(sol)} \qquad (6)$$

where $Org_{(ads)}$ is the organic specie adsorbed on to the solid state (metal), $H_2O_{(ads)}$ is the water molecule adsorbed on the solid state surface and *x* is the number of water molecules replaced by one organic inhibitor adsorbate.

It is well known that the chemical structures of inhibitor molecules strongly effect on adsorption of these molecules on the solid state[45]. So, adsorption isotherms were drawn for determining the related mechanism. The most common isotherms are those developed by Langmuir, Frumkin, Hill de Boer, Temkin, Flory Huggins and El-Awady-Abd–El-Nabey-Aziz[45]. All these isotherms are of the general form:

$$f(\theta, x)\exp(-sa\theta) = K_{ads.}C \qquad (7)$$

where f(θ, *x*) is the configurational factor depends upon the physical model[46], θ surface coverage degree, C the concentration of organic compound in the test solution, *x* the size ratio, *a* the molecular interaction, and $K_{ads.}$ is the equilibrium constant of the adsorption process.

Linear relationship for plots of θ against logC_{inh} in **Fig.(6)** with r^2>0.90 shows that adsorption data fitted Temkin adsorption isotherm, **Eq. 8**.

$$\theta = \frac{-2.303 log K}{2a} - \frac{2.303 log\ Cinh.}{2a} \qquad (8)$$

Adsorption parameters obtained from this isotherms and the free energy of adsorption (ΔG_{ads}) calculated according to**Eq. 9** are recorded in **Table 7** .

$$\Delta G_{ads.} = -2.303RT \log(55.5K) \qquad (9)$$

The highly value of $K_{ads.}$ and more inactive value of ΔG_{ads} for $\mathbf{H_2L^2}$ reflect the highly adsorption capability and spontaneous adsorption of the $\mathbf{H_2L^2}$ molecule on cast iron surface. According to the negative sing of attractive parameter (a), adsorption layer suffer some repulsion between the Schiff base molecules.

The organic molecules can adsorbed onto the solid state through several active groupes in their structure. In the case of tow Schiff base, H_2L^1 and H_2L^2, efficient adsorption is the result of some factors as π electrons of double bonds and aromatic system, nitrogen, sulphur, oxygen electronegative atoms and C=N, C=O or C=S groups which are present in the structures. Also it is well knownthat iron has coordination affinity towards nitrogen, oxygensulphurbearing ligands[47,48]. The free electron pairs in these atoms are capable of forming acoordination σbond with iron[49]. Among these tow Schiff base, the chelate effect is highest in $\mathbf{H_2L^2}$ as the position of thetetradentate ligand so shows an inhibition efficiency of 94.3% and 93.3%. Efficient adsorption in this compound is the result of tow C=N groups beside C=S and C=O groups present in the structure. The doner atoms (O,N,S) in these groups are very suitable for σ bond in iron. The same result was estimated by Hosseini et al.[49] and Shokry et al.[50], where the inhibitive effect of some asymmetric Schiff base ligandswith tetradentate coordination sites has been shown to act as effective inhibitors for mildsteel in 1M HCl and 0.5 M H_2SO_4 media respectively.The difference in the inhibition efficiency also lies mostly in the size of organic compound; H_2L^1 with lower size than H_2L^2 and tridentate being less effective.

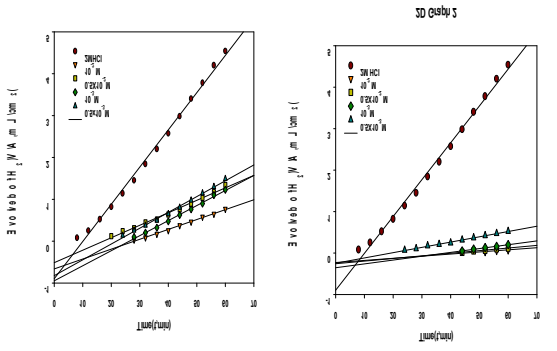

Fig.5: Hydrogen evolution during cast iron corrosion in 2.0M HCl +10% MeOH in absence and presence schiff base compounds at 30 C.

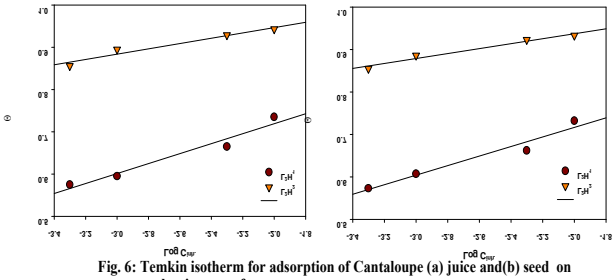

Fig. 6: Temkin isotherm for adsorption of Cantaloupe (a) juice and(b) seed on aluminum surface

3.10 Antimicrobial activity

The antibacterial and antifungal activity of the ligands and their metal complexes were tested against *gram-positive*, *gram-negative* bacteria and fungi using a modified Kirby-Bauer disc diffusion method[24]. The biological activity data were founded in Table 8 and 9. The prepared complexes have remarkable bactericidal and fungicidal properties compared with the parent ligands due to the effect of metal ions on the normal cell process and the lipophilic character of the metal complexes [51]. The activities of the metal complexes could also be understood in terms of chelation theory[52].$[(HL^1)_2Hg(H_2O)_2]2H_2O$complexshowed higher range of inhibition diameter thanAmpicillin(Antibacterial agent), Amphotericin B(Antifungal agent) and other complexes. The other complexes have less activity against different microorganisms depends either on kinds of metal ions and the ability of the cells ofmicrobes or difference in ribosomes of microbial cells [53, 54].

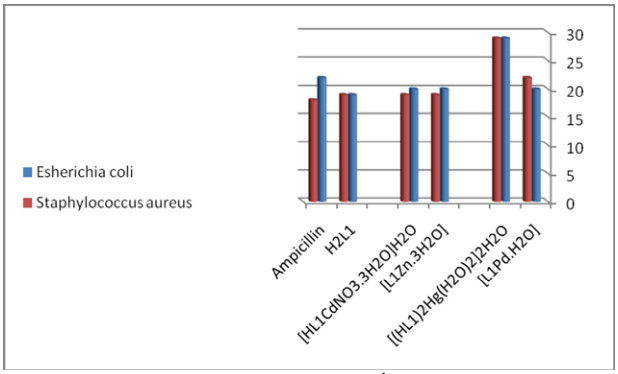

Fig.7: Antibacterial activity of the ligand(H_2L^1) and their complexes.

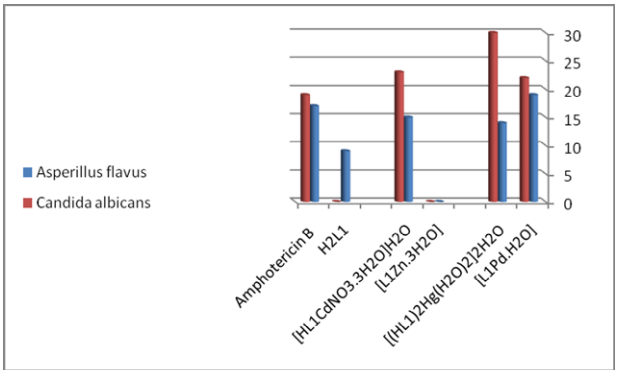

Fig.8: Antifungal activity of the ligand (H_2L^1) and their complexes.

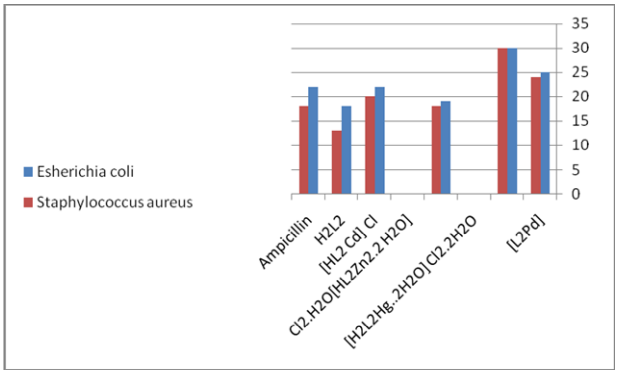

Fig.9: Antibacterial activity of the ligand(H_2L^2) and their complexes.

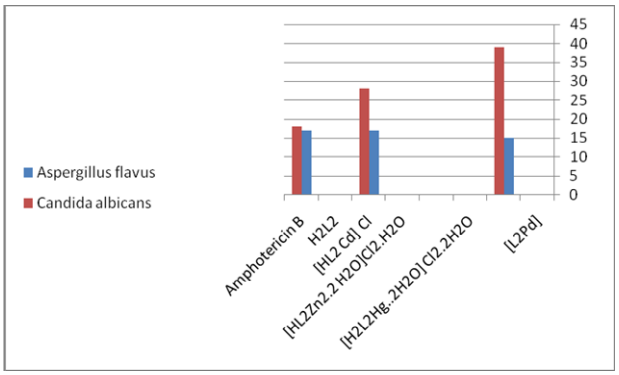

Fig.10: Antifungal activity of the ligand (H_2L^2) and their complexes.

CONCLUSION

N-(2-hydroxyphenyl)-3-(2-hydroxyphenylimino) butanamid and ethylacetoacetate –isonocotinoyl thiosemicarbaziedhydrazone Schiff bases(H_2L^1) and (H_2L^2) were synthesized and characterized. Their inhibition efficiencies obtained from both MLM and HEM methods are in good agreement. Defferences in inhibition rfficiency between H_2L^1 and $H_2L^2$are correlated with their chemical structurs. The Palladium(II), mercury(II), cadimum(II) and zinc(II) complexes have been synthesized and characterized and screened for their antimicrobial activities using amodified Kirby- Bauer disc diffusion method. .$[(HL^1)_2Hg(H_2O)_2]2H_2O$complexshowed higher range of inhibition diameter than Ampicillin(Antibacterial agent) , Amphotericin B(Antifungal agent) and other complexes.

ACKNOWLEDGMENT

The authors gratefully acknowledge Qassim University, represented by the Deanship of Scientific Research, on the material support for this research under the number (**2884**) Sabic grant .

REFERENCES

[1] L.S. Mcneiill, M. Edwards, Journal-American Water Works Association 93(7)(2001), 88-100.
[2] F. Teng; Y.T. Guan; W.P. Zhu, Corr. Sci., 2008, 50(10), 2816.
[3] A.G. Macdonald, F.H. Stott, Corros. Sci., 1988, 28(5), 485.
[4] V.Rajeswari, D.Kesavan, M.Gopiraman, P.Viswanathamurthi, K.Poonkuzhali, T.Palvannan, Appl. Surf. Sci., 2014, 314(30), 537.
[5] M. Abdallah, Corros. Sci., 2002, 44, 717.
[6] Asan, M. Kabasakalog˘lu, M. Is kalan, Z. Kılıc, Corros. Sci., 2005, 47, 1534.
[7] S.T. Arab and K. M. Emran, Int. J. Appl. Chem., 2007, 3, 69.
[8] S.T. Arab, K.M. Emran, Mater. Lett., 2008, 62, 1022.
[9] M.A. Hegazy, Corros. Sci., 2009, 51, 2610.
[10] Y. Tang, X. Yang, W. Yang, Y. Chen, R. Wana, Corros. Sci., 2010, 52, 242.
[11] N. A. Wazzan, J. Ind.& Eng. Chem., 2015,26, 291.
[12] Y.K. Agrawal, J.D. Talati, M.D. Shah, M.N. Desai, N.K. Shah, Corros. Sci. 2004, 46 515.
[13] S.M. Shaban, A. Saied, S.M. Tawfik, A. Abd-Elaal, I. Aiad, J. Ind. Eng. Chem. 2013,19 ,2004.
[14] Xu, W. Yang, Y. Liu, X. Yin, W. Gong, Y. Chen, Corros. Sci., 2014, 78, 260.
[15] S.T. Arab, E.A. Noor, Corrosion, 1993, 49,122.
[16] L.A. Raspi, Nickel Corros. 1993, 49 821.
[17] D.N. Singh, A.K. Dey, Corrosion, 1993, 49, 594.
[18] G. Banerjee, S.N. Malhotra, Corrosion, 1992, 48, 10.
[19] G. Cerchiaro, K. Aquilano, G. Filomeni, G. Rotilio, M.R. Cirioio, A.M.D.C. Ferreira, J. Inorg. Biochem., 2005, 99, 1433.
[20] J. Vancoa, O. Svajlenova, E. Racanskac, J. Muselika, J. Valentova, 2004 Journal of Trace Elements in Medicine and Biology 18 155.
[21] Aiad, N. Negm, J. Surfact. & Deterg., 2009, 12, 313.
[22] M. Calligaris, L. Randaccio and G. Wilkinson, Comprehensive Coordination Chemistry, PergamonPress, Oxford, 1987.
[23] B.R. Thorat, P. Kamat, D. Khandekar, S. Lele, M. Mustapha, S.Sawant, R. Jadhav, S. Kolekar, R. Yamga, R.G.Atram, *J. Chem. Pharm. Res.*, 2011, 3(6), 1109.
[24] A.W. Bauer, W.M. Kirby, C. Sherris, M. Turck, Am. J. Clin. Pathol., 1966, 45, 493.
[25] National Committee for Clinical Laboratory Standards. Methods for dilution antimicrobial susceptibility tests for bacteria that grow aerobically. 4th ed. Approved standard M7-A4. Wayne, Pa: National Committee for Clinical Laboratory Standards; 1997.
[26] M.N. Mookerjee, R.V .Singh, J.P. Tandoti, Tmns. Met. Chem., 1985, 10, 66.
[27] R. K. Mahapatra, B. K. Mahapatra and S. Guru, J. Inorg. Nucl. Chem., 199739, 2281.
[28] K.Nakanishi, Infrared Absorption Spectroscopy", Holden-Day Inc.San Francisco, 1962.
[29] N. B. Colthup, L. H. Daly, S. E.Wiberly, "Introduction to Infrared
[30] and Raman Spectroscopy", Academic Press, , 2nd Ed., New York, 1975.
[31] K. Nakamato, "Infrared Spectra of Inorganic and Coordination
[32] Compounds", John Wiley, 2nd Ed., New York, 1966.
[33] Y. He, B. Wu, J.Yang , D. Robinson, L. Risen, R. Ranken , Bioorg
[34] Med. Chem. Lett., 2003, 13, 3253.
[35] Klimesova, J. Koci, K. Waisser, J. Kaustova, New benzimidazole
[36] derivatives as antimycobacterial agents. Farmaco 2002, 57, 259.
[37] Z. El-Sonbati, Transition Met. Chem.1991,16, 45.
[38] A.W. Baker, A.T. Shulgin, J. Am. Chem. Soc., 1959, 81,1523.
[39] M. Nath, M. Sulaxna, X. Song, G. Eng, J. Organomet.Chem., 2006,691,1649.
[40] V.M Leovac, G.A. Bogdanović, V.I. Češljević, L.S. Jovanović, S.B. Novaković, L.S. Vojinović-Ješić, Struct.Chem., 2007,18,113.
[41] M. Nath, M. Sulaxna, X.Q. Song, G. Eng Spectrochim.Acta, 2006, 64A,148.
[42] W.J.Geary, Coord. Chem. Rev. ,1971,7,81.

[43] E. E. Ebenso, E. E. Oguzie, Mater. Lett., 2005, 59, 2163.
[44] R. Solmaz, G. Kardaş, B. Yazici, M. Erbil, Colloids Surf. A Physicochem. Eng. Asp., 2008 312,7.
[45] K. M. Emran, A. O. Al-ahmadi, B. a Torjoman, N. M. Ahmed, S. N. Sheekh, African J. Pure Appl. Chem., 2015 9,39.
[46] P.C. Okafor, U. J.Ekpe, E. E.Ebenso, E. M. Umoren, K. E. Leizou, Bull. Electrochem., 2005, 21, 347.
[47] A.O. Odiongenyi, S.A. Odoemelam, N.O. Eddy, Portugalia Electroch. Acta, 2009, 27(1), 33.
[48] O. N. Eddy, B.I. Ita , N.E. Ibisi , E. E. Ebenso, Int. J. Electrochem. Sci., 2011, 6, 1027.
[49] J.M. Bastidas, P. Pinilla, E. Cano, J.L. Polo, S. Miguei, Corros. Sci., 2003 , 45 427.
[50] Ateya, B. El-Anadouli, F. El-Nizamy, Corros. Sci., 1984, 24, 509.
[51] B.S. Snyder, G.S. Patterson, A.J. Abrahamson, R.H. Holm, J. Am. Chem. Soc., 1989, 111, 5214.
[52] S.T.Arab and K.M.Emran, J. Saudi Chem. Soc., 2006, 10,19.
[53] M. Hosseini, S.F.L. Mertens, M. Ghorbani, M.R. Arshadi, Mater. Chem. Phys., 2003, 78, 800.
[54] H. Shokry, M. Yuasa, I. Sekine, R.M. Issa, H.Y. El-Baradie, G.K. Gomma, Corros. Sci., 1998, 40, 2173.
[55] P.G.Ramappa, , K. G.Somashekarappa, J. Inorg. Biochem., 1994 55, 13.
[56] R.S. Srivastava, Inorg. Chim. Acta, 1981,56, L65.
[57] N.Sari, S.Arslan, E.Logoglu, L. Sakiyan, J. Animal Sci., 2003,16, 283.
[58] Jayabalakrishnan, K. Natarajan, Transit. Met. Chem, 2002, 27, 75

Table 1: Chemical compositions of cast iron specimen with weight percentage(%W).

%C	%Si	%Mn	%P	%S	Remain
3.45 - 3.65	2.40 - 2.70	0.60 – 0.70	0.17 – 0.26	0.04 – 0.06	Fe

Table 2 :^{1}HNMR spectra data of the ligands and its cadmium complexes.

Compounds	Chemical shift (δ) ppm					
	NH	OH	Ar or Py	CH_2	CH_3	CH
(H_2L^1)	9	4.5	6.4-7	3.5	2.5	-
$[HL^1CdNO_3.3H_2O]H_2O$	9	4.7	6.4-7	3.4	2.5	
(H_2L2)	4.5,8.0	10.1	7.7, 8.7	4.1, 3.6	1.1, 2.0	-
$[HL^2$ Cd Cl]	4.5	-	7.7, 8.7	4.1, 3.5	1.1, 2.0	1.8

Table 3: Analytical and physical data of the ligands and their complexes.

No.	compound	colour	M.wt	M.P°C	Yield%	Anal.found (Calc.)%				
						%C	%H	%N	%M	%S
1	$H_2L^1(C_{16}H_{16}N_2O_3)$	Pale brown	284	185	85	67.8 (67.6)	5.6 (5.6)	9.0 (9.8)	-	-
2	$[HL^1Cd(NO_3).3H_2O]H_2O$	Brown	512.4	300>	90	36.6 (36.2)	3.9 (4.3)	7.5 (7.9)	21.5 (21.9)	-
3	$[L^1Zn.3H_2O]$	Brown	401.4	300>	92	47.9 (47.8)	5.4 (5.0)	7.7 (7.0)	17.0 (16.3)	-
4	$[(HL^1)_2Hg(H_2O)_2]2H_2O$	Brown	840.6	300>	80	45.4 (45.7)	4.8 (4.5)	6.4 (6.7)	23.5 (23.8)	-
5	$[L^1Pd.H_2O]$	Deep Brown	406.4	270	80	47.0 (47.2)	3.5 (3.9)	6.5 (6.6)	(26.2)	-
6	$H_2L^2(C_{13}H_{18}N_6O_2S)$	yellow	322	110	95	48.0 (48.4)	5.2 (5.6)	25.7 (26.0)	-	9.8 (9.9)
7	$[HL^2Cd]Cl$	White	468.9	280	90	33.6 (33.3)	3.9 (3.6)	18.0 (17.9)	24.3 (24.0)	6.9 (6.8)
8	$[L^2Zn_2.2H_2O]Cl_2.H_2O$	Deep yellow	576.3	300>	85	27.2 (27.1)	2.9 3.2)	14.9 (14.6)	22.2 (22.7)	5.8 (5.6)
9	$[H_2L^2Hg..2H_2O]\ Cl_2.2H_2O$	Pale yellow	664.6	300>	90	23.8 (23.5)	3.5 (3.6)	12.9 (12.6)	30.0 (30.2)	5.0 (4.8)
10	$[HL^2Pd]Cl$	Brown	462.9	260	80	33.2 (33.7)	3.5 (3.7)	18.7 (18.1)	22.4 (22.9)	7.4 (7.5)

Table 4: IR Spectra of the ligands and their complexes.

Table 5: UV Spectral data and DTA analysis of the prepared ligands and their complexes.

No.	Molecular Formula Compounds	UV Spectra λ_{max}(nm) keto-imine form	OHν n-π*	NHν π-π*	C-T	C=Oν TG Peaks Temp.°C	wt lost %(calc.)found	νC=N Peak	C=Sν	νM-O Temp.°C	DTA Peaks
1	$H_2L^1(C_{16}H_{16}N_2O_3)$	433,414	3481(s) 3370(s) 346,328,317,309	3302(s) 299,291,280	-	1727(s) 100-210 390-490	1588(s) 93.9 4.5	- Endo. Exo.	-	- 175 469.38	
2	$[HL^1CdNO_3.3H_2O]H_2O$	435	3374(s) 302	3300(m) 290,284	502	- 125-150 200-240 300-450 500-600	1610(s) (3.4)3.5 (6.8)7.0 (11.9)11.5 60	- Endo. Exo. Endo.	-	145.5 234.17, 234.78 399.7 589(m)	52
3	$[L^2Zn.3H_2O]$	432	3297(s) 300	3238(s) 294,249	502	1606(s)					53
4	$[(HL^1)_2Hg(H_2O)_2]2H_2O$	435	3374(s) 304,300	3303(s) 289,279	502	- 160-250	1601(s) (13.5)13.0	- Endo.	-	583(m) 171.49	54
5	$[L^1Pd.H_2O]$	464,425,414,404	3343(s) 397,390,357,325	3262(s) 292,278	502	400-660 600-780	1596(s) 55.6 5.5	Exo. Endo.	-	582(m) 602.78 769.75	53
6	$H_2L^2(C_{13}H_{18}N_6O_2S)$		3481(s)	3364(s) 3241(s)		1727(s) 120-185 200-240	1664(s) 1578(s) (4.3)4.1 (4.3) 4.0	742 Endo. Endo.		184.62 233.18	
7	$[HL^2Cd]Cl$		3419(w)	3320(s)		1691(s) 400-510 550-660	1618(s) 40-5 1554(m) 10.7	Exo. Exo. Exo.	-	449.87 662(m) 581.18 651.87	54
8	$[L^2Zn_2.2H_2O]Cl_2.H_2O$		3425(br)	3236(s)		- 200-240	1656(s) 1600(s) (4.4)4.2	Endo.	-	557(m) 227.55	46
9	$[H_2L^2Hg..2H_2O]\ Cl_2.2H_2O$		3458(br)	3310(s)		1681(s) 240-445	1636(s) 30.9 5.4 1551(m) 6.2	Endo. Exo. 693 Exo.		240.04 604(m) 503 435	53
10	$[HL^2Pd]Cl$		3343(s)	3254(s)		-	1634(s) 1608(s)	690		599(s)	45

6	$H_2L^2(C_{13}H_{18}N_6O_2S)$		300		289,226	117-200 200-300 300-372 374-614 615-799	19.3 38.8 24.6 6.9 3.0	Endo. Exo. Exo. Exo.	85.64, 116.82 164.53, 242.69 323.61, 450.82 605.13	
7	$[HL^2\ Cd]\ Cl$		310		284,280	280-330 400-620	20.4 30.6	Endo. Exo. Exo.	313.19 469.44 587.60	
8	$[L^2Zn_2.2\ H_2O]Cl_2.H_2O$		321,310,300		287	230-250 270-350 400-660	(3.1) 3.0 (12.3)12.1 26.5 12.3	Exo. Exo. Endo. Exo. Exo.	245.51 340.66 420.66 480.31, 564.13 654.46	
9	$[H_2L^2Hg..2H_2O]Cl_2.2H_2O$	H_2L^1 H_2L^2	287,2 305 78		287,2	80-120 200-233 73.2 275-355 400-730	(2.7)2.5 (5.4)5.0 10.8)10.0(88.0 92.3 93.3	Endo. Endo. Endo. Endo. Endo. Endo.	101.14 227.15, 240.24 330.8 727.01	
10	$[HL^2Pd]Cl$		310		270	200-290 300-685	(7.8) 7.1 20.5	Endo. Exo.	281.12 393.19,681.37	

Table 6 : Action inhibition of compunds in 2.0M HCl+10% MeOH at 30°C.

$C_{inh.}$ (mol/L)	HEM R_{HEM} (ml.cm^{-2}.min)	HEM %η	HEM θ	MLM R_{MLM} (mg.cm^{-2}.min)	MLM %η	MLM θ	mmy
Blank	0.0889	-	-	1.417×10^{-4}	-	-	0.27
0.5×10^{-3}	0.0378	57.5	0.575	6.050×10^{-5}	57.3	0.573	1.15×10^{-2}
1.0×10^{-3}	0.0360	59.5	0.595	5.568×10^{-5}	60.7	0.607	1.06×10^{-2}
0.5×10^{-2}	0.0298	66.5	0.665	4.974×10^{-5}	66.2	0.662	3.19×10^{-3}
1.0×10^{-2}	0.0236	73.5	0.735	3.797×10^{-5}	73.2	0.732	7.29×10^{-3}
0.5×10^{-3}	0.0128	85.6	0.856	2.061×10^{-5}	85.5	0.855	3.95×10^{-3}
1.0×10^{-3}	0.0093	89.5	0.895	1.611×10^{-5}	88.6	0.886	3.09×10^{-3}
0.5×10^{-2}	0.0063	92.9	0.929	1.090×10^{-5}	92.3	0.923	2.09×10^{-3}
1.0×10^{-2}	0.0051	94.3	0.943	9.549×10^{-6}	93.3	0.933	1.29×10^{-3}

Table (7): Adsorption parameters for adsorption of aluminum surface in mass loss and hydrogen evaluation measurements:

Schiff Base	*H_2 evolution method (HEM)*				*Mass loss method (MLM)*			
	R^2	LogK	$\Delta G°_{ads}$ ($kJmol^{-1}$)		R^2	LogK	$\Delta G°_{ads}$ ($kJmol^{-1}$)	
L_2H^1	0.95	8.10	-55.36	a= -9.77	0.989	8.37	-56.88	a=-10.23
L_2H^2	0.96	17.1	-105.97	a=- 18.3	0.999	18.05	-111.32	a=-19.72